

# PROCEEDINGS OF SPIE

[SPIDigitalLibrary.org/conference-proceedings-of-spie](https://spiedigitallibrary.org/conference-proceedings-of-spie)

## High-Q optical nanocavities in planar photonic crystals

Jelena Vuckovic, Marko Loncar, Tomoyuki Yoshie, Axel Scherer, Michael Armen, et al.

Jelena Vuckovic, Marko Loncar, Tomoyuki Yoshie, Axel Scherer, Michael Armen, Jon Williams, Hideo Mabuchi, "High-Q optical nanocavities in planar photonic crystals," Proc. SPIE 4629, Laser Resonators and Beam Control V, (6 June 2002); doi: 10.1117/12.469495

**SPIE.**

Event: High-Power Lasers and Applications, 2002, San Jose, California, United States

# High-Q optical nanocavities in planar photonic crystals

Jelena Vučković, Marko Lončar, Tomoyuki Yoshie and Axel Scherer  
Michael Armen, Jon Williams and Hideo Mabuchi

Departments of Electrical Engineering and Physics  
California Institute of Technology, 136-93  
Pasadena, CA 91125, U.S.A.

## ABSTRACT

Planar photonic crystals are constructed by combining two-dimensional periodic structures with high refractive index contrast slabs. By suppressing the loss in these structures due to imperfect confinement in the third dimension, one can fully take advantage of their relatively simple fabrication, and achieve the functionality of three-dimensional photonic crystals. One of the greatest challenges in photonic crystal research is a construction of optical nanocavities with small mode volumes and large quality factors, for efficient localization of light. Beside standard applications of these structures (such as lasers or filters), they can potentially be used for cavity QED experiments, or as building blocks for quantum networks. This paper will address our theoretical and experimental results on optical nanocavities based on planar photonic crystals, with mode volumes as small as one half of cubic wavelength of light in material, and with Q factors even larger than  $1 \times 10^4$ .

**Keywords:** photonic crystals, nanocavity, FDTD methods, cavity QED, Q factor

## 1. INTRODUCTION

Photonic crystals (PCs) are structures with periodic variation of dielectric constant in one, two or three dimensions.<sup>1-5</sup> This periodicity is usually of the order of the wavelength of light in material that the PC is made of. While the one-dimensional structures operating at optical wavelengths have been known for more than 20 years,<sup>1</sup> the extension of photonic crystals to two and three dimensions was simultaneously proposed by Yablonovitch and John in 1987.<sup>2,3</sup> Although 3D PCs offer the opportunity of light manipulation in all three dimensions in space, they are very difficult to fabricate.<sup>6</sup> For this reason, many research groups have concentrated their efforts on planar photonic crystals (i.e., 2D photonic crystals of finite depth) in recent years.<sup>7-17</sup> By introducing point or line defects into such 2D PC arrays, a variety of passive and active optical devices can be constructed, and integrated on a single chip. The fabrication procedures of planar PCs are much simpler than those of their 3D counterparts, but their light confinement is only "quasi-3D," and resulting from the combined action of 2D photonic crystal and internal reflection. The imperfect confinement in the third dimension produces some unwanted out-of-plane loss (radiation loss), which is usually a limiting factor in performance of these structures.

One of the most important properties of photonic crystals is their ability to localize light into small mode volumes. Even the simplest single defect nanocavities in planar photonic crystals with triangular lattice, produced by changing the radius or refractive index of a single PC hole or rod, can localize light into the volumes as small as one half of cubic wavelength in material. Unfortunately, these most obvious nanocavity designs have maximum quality factors of the order of only a few thousand.<sup>8,18-20</sup> However, our group at Caltech has recently proposed the design and fabrication of optical nanocavities based on free-standing membranes, with  $Q > 10^4$  and mode volumes still of the order of one half of cubic wavelength of light in material.<sup>8,21,22</sup> We have also recently demonstrated the experimental Q factor of 2800 in this type of structure, for which the theoretically predicted Q was around 4000.<sup>23</sup> The topic of this article is the design, fabrication and characterization of these novel structures. Beside standard applications (such as optical filters, or laser resonators), they can also be used for achieving spontaneous emission control, threshold-less lasing, or as building blocks for quantum networks.<sup>8,24</sup>

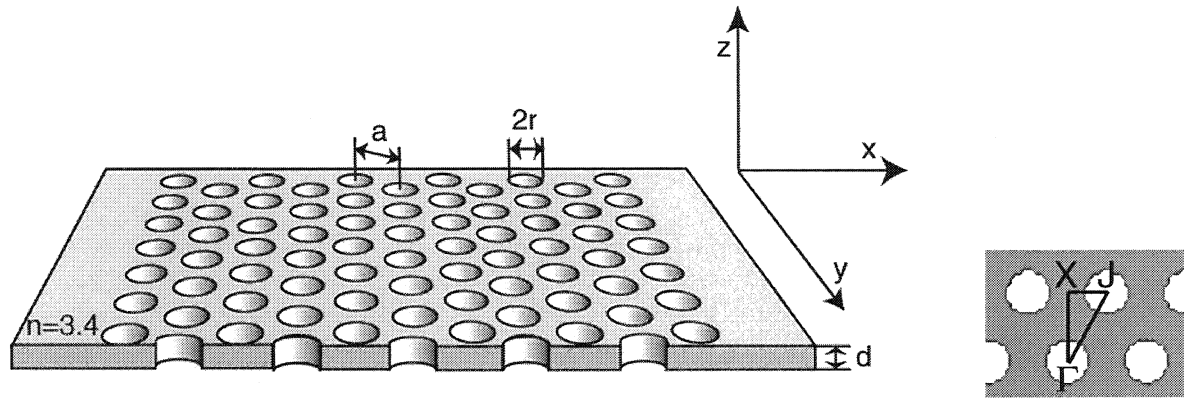


**Figure 1.** Optically thin membrane patterned with a triangular array of air holes.

## 2. THEORY

### 2.1. Choice of photonic crystal parameters

The first step in the structure design is the choice of PC parameters. There are five parameters that we can control, as illustrated in Figure 1: the refractive index of material ( $n$ ), the type of photonic crystal lattice (triangular, square...), the thickness of the slab ( $d$ ), the lattice periodicity ( $a$ ), and the hole radius ( $r$ ). The wavelength of light in air is denoted as  $\lambda$ . Since our structures are usually made out of Si or III-V semiconductors, we do not have much choice over the refractive index, which is in the range between 3.4 and 3.5. Furthermore, we concentrate mostly on triangular lattice crystals, which can provide us with a better lateral confinement than square lattice crystals.<sup>25</sup> However, properties of PC are still very sensitive to the remaining three parameters:  $d$ ,  $r$  and  $a$ . TE-like modes (also referred to as the even modes) have dominant  $E_x$ ,  $E_y$  and  $B_z$  components in the middle of the slab. It is important to note that the structures presented here do not have a bandgap for TM-like (odd) modes (having the dominant  $B_x$ ,  $B_y$  and  $E_z$  components in the middle of the slab).

As mentioned previously, parameters of the band diagram are highly sensitive to  $d$ ,  $r$  and  $a$ . Figure 2 illustrates how the TE bandgap edges shift in frequency as a function of  $d/a$  and  $r/a$ , in the case of the triangular lattice with  $n = 3.5$ . The control over a position of a bandgap by tuning  $r/a$  and  $d/a$  is a very powerful property of planar PCs, which implies that one can tune mirrors by lithography and etching, instead of growth. Furthermore, mirrors operating at many different wavelengths can be constructed on the same chip. Therefore, if  $d/a$  increases, but  $r/a$  is kept constant, the band edges shift downwards in frequency and bandgap size remains approximately constant in the analyzed range. On the other hand, if  $d/a$  is kept constant, but  $r/a$  increases between 0.3 and 0.4, the bandgap edges shift upwards in frequency and the bandgap size increases. Even though the increase in the hole size leads to the increase of the bandgap, which is desirable for suppression of lateral loss, it also produces large out-of-plane losses. For this reason, we limit  $r/a$  of our structures to rather modest values of around 0.3. Since the reduction in  $r/a$  leads to a decrease in the size of the bandgap, it is important not to reduce the hole radius too much, in order to preserve the lateral confinement and small mode volume (e.g., we do not use  $r/a$  below 0.275). The  $d/a$  ratio of our structures is usually between 0.65 and 0.75, and we were able to design nanocavities with very high Q factors at both ends of this range, without a significant change in the mode volume.<sup>8,24</sup> The reasons for choosing this thickness range are the following: if the slab is too thin, the mode is not confined well within it vertically, and it interacts more strongly with the substrate (positioned at around  $\lambda/2$  underneath the bottom membrane surface in our structures<sup>8</sup>), which reduces its Q factor. Furthermore, the fabrication of very thin suspended membranes is difficult, and these structures are not very robust. On the other hand, if  $d/a$  is too large, the structure is multimode in the vertical direction, which is also undesirable.

The nanocavities presented in this article are based on the following two sets of parameters: (1)  $n=3.4$ ,  $d/a=0.75$  and  $r/a=0.275$ ; (2)  $n=3.4$ ,  $d/a=0.65$  and  $r/a=0.3$ . The band diagrams for TE-like modes in the planar PCs with

Further author information: Send correspondence to Jelena Vučković. E-mail: jela@caltech.edu

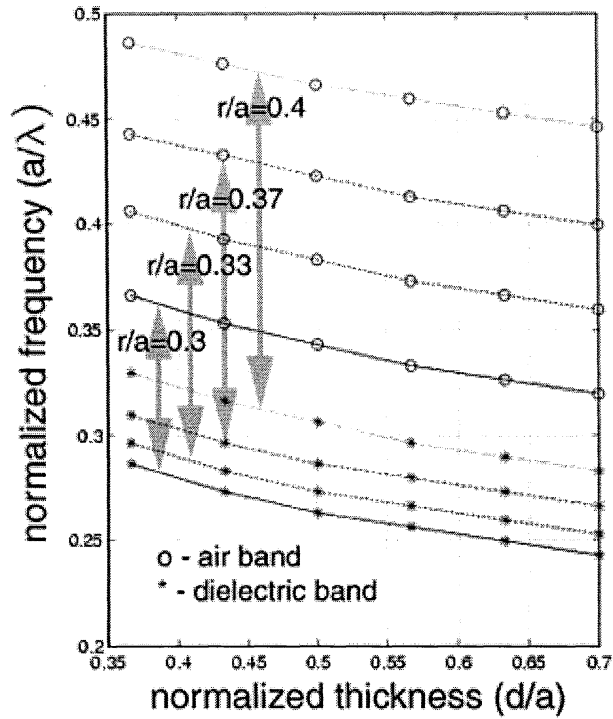


Figure 2. Position and size of the bandgap as a function of  $d/a$  and  $r/a$  in the triangular lattice with  $n=3.5$ .

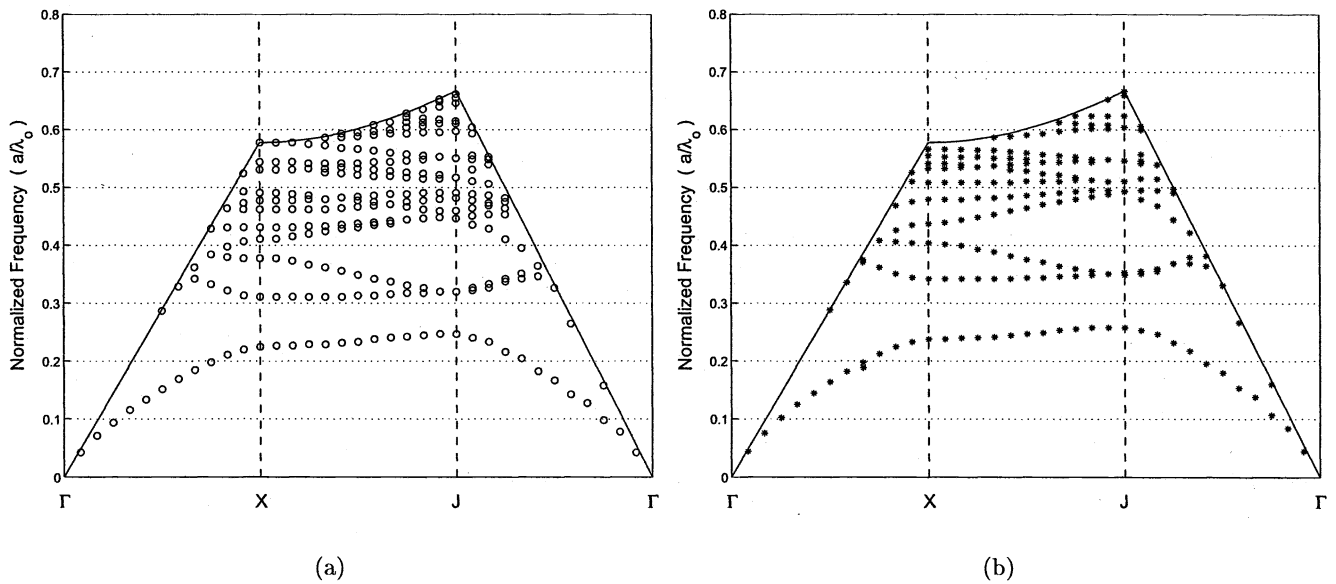
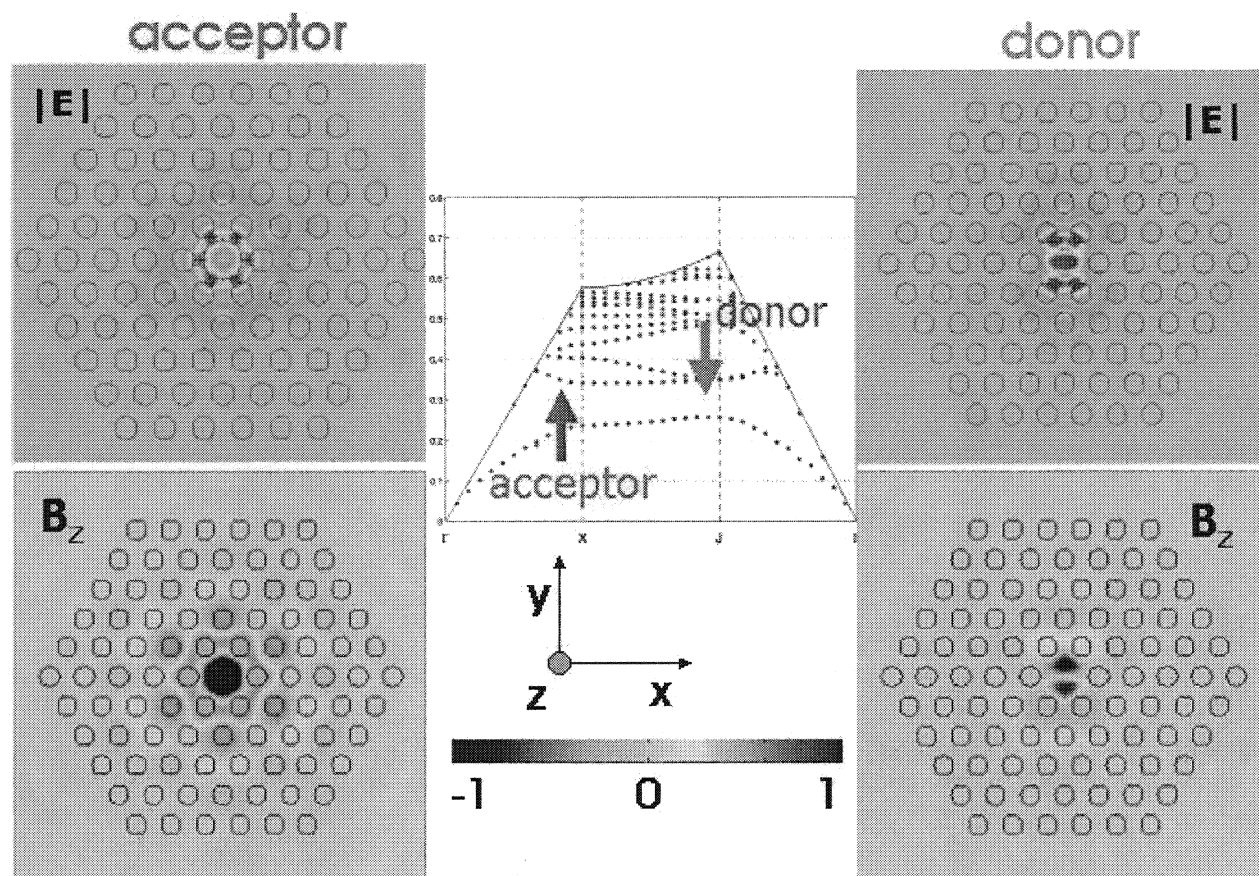


Figure 3. Band diagrams for TE-like modes of a thin slab surrounded by air on both sides and patterned with a triangular array of air holes. Parameters of photonic crystal are (a)  $n=3.4$ ,  $d/a=0.75$  and  $r/a=0.275$ ; (b)  $n=3.4$ ,  $d/a=0.65$  and  $r/a=0.3$ .

these parameters are shown in Figure 3. In the FDTD method, we apply the discretization of 20 pixels per periodicity  $a$ .

## 2.2. Point defects in planar photonic crystals

The simplest way of forming a nanocavity starting from the photonic bandgap (PBG) structure shown in Figure 1 is by changing the radius of a single hole, or by changing its refractive index. The former method is more interesting from the perspective of fabrication, since lithographic tuning of parameters of individual holes is a simple process to implement. By increasing the radius of a single hole, an acceptor defect state is excited, i.e., pulled into the bandgap from the dielectric band. On the other hand, by decreasing the radius of an individual hole (or by tuning its refractive index between 1 and the refractive index of the slab), a donor defect state is excited and pulled into the bandgap from the air band.<sup>26</sup>



**Figure 4.** Acceptor defect state (monopole) and donor defect state (dipole) excited by changing the radius of a single PC hole.

Acceptors tend to concentrate their electric field energy in regions where the large refractive index was located in the unperturbed PC, while the electric field energy of donors is concentrated in regions where there was air in the unperturbed PC, as shown in Figure 4. The donor defect state shown in Figure 4 is called a dipole mode. This mode has a double degeneracy<sup>27</sup> and can be separated into the  $x$  and  $y$  dipole modes, based on the orientation of the electric field in the center of the defect.

The total loss that a defect state suffers can be separated into the lateral (in-plane) loss, and vertical (out-of-plane) loss. Similarly, the total quality factor of a defect mode can be expressed as a superposition of lateral and vertical

quality factors:

$$\frac{1}{Q} = \frac{1}{Q_{\parallel}} + \frac{1}{Q_{\perp}}. \quad (1)$$

$Q_{\parallel}$  and  $Q_{\perp}$  are inversely proportional to the lateral and vertical losses, respectively. In all of our calculations, the boundary for separation of vertical from lateral loss (i.e., the vertical quality factor  $Q_{\perp}$  from the lateral quality factor  $Q_{\parallel}$ ) is positioned approximately at  $\lambda/2$  from the surface of the membrane. For structures operating at bandgap frequencies,  $Q_{\parallel}$  increases as the number of PC layers around the defect increases, and the total quality factor  $Q$  approaches  $Q_{\perp}$ .<sup>8</sup> The vertical quality factor ( $Q_{\perp}$ ) saturates after around five PC layers surrounding the defect. For our calculations, we also assume that  $x = 0, y = 0, z = 0$  denotes the center of the cavity and  $z = 0$  is the middle plane of the slab. For all presented analyses, five layers of PC holes surround the defect and the applied discretization of  $a = 20$  points per lattice periodicity was used.

The simplest single defect nanocavities in planar photonic crystals with triangular lattice, produced by changing the radius or refractive index of a single PC hole or rod, can localize light into the volumes as small as one half of cubic wavelength in material. Unfortunately, these most obvious nanocavity designs have maximum quality factors of the order of only 2000.<sup>8,18-20,24</sup> This was, clearly, not good enough for some of the applications that we had in mind (such as cavity QED), for which reason we initiated our work on designing a nanocavity that could still localize light into such a small volume, but have a much larger  $Q$  factor. Some of our successful designs will be presented in the next Subsection of this article.

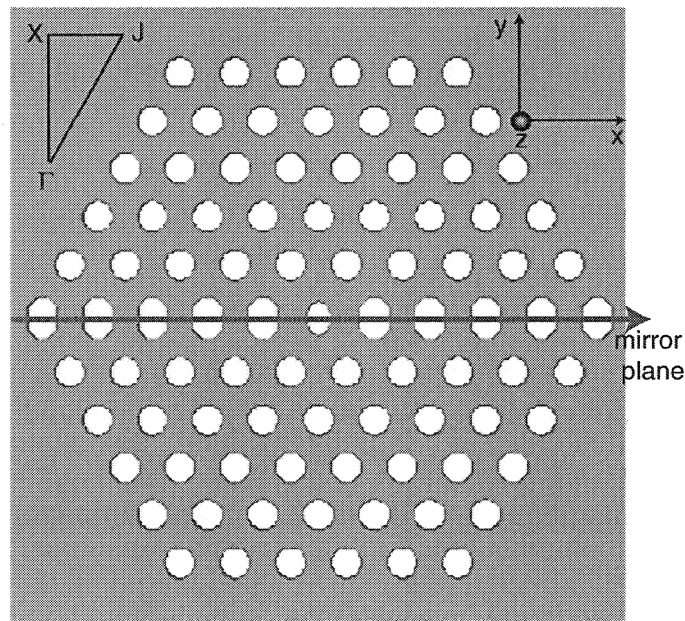


**Figure 5.** Microcavity structure consisting of a single defect (produced by reducing the radius of the central hole to  $r_{def}/a = 0.2$  from  $r/a = 0.275$ ) and a fractional edge dislocation of order  $p = 4$  along the  $x$  axis. The applied discretization is 20 pixels per periodicity  $a$ .

### 2.3. Design of high $Q$ optical nanocavities: fractional edge dislocations in planar photonic crystals

We have recently proposed the design and fabrication of optical nanocavities in free standing membranes with  $Q > 10^4$  for the dipole mode, and mode volumes of the order of one half of cubic wavelength of light (measured in material).<sup>8,21</sup> The dramatic improvement in  $Q$  factors over single defect nanocavities (without a significant increase in the mode volume) was obtained by introducing a novel type of photonic crystal lattice defect, consisting of the elongation of holes along the symmetry axes. We call this type of defect a *fractional edge dislocation*, by analogy with edge dislocations in solid state physics. Edge dislocations are formed by introducing extra atomic planes into

the crystal lattice. On the other hand, we here insert only fractions of atomic planes along the symmetry axes of photonic crystal, as shown in Figure 5. Hole-to-hole distances are preserved under this deformation, and the half-spaces  $y > p/2$  and  $y < -p/2$  maintain the unperturbed photonic crystal geometry.

We start from the triangular photonic crystal with the previously introduced parameters, and reduce the central hole radius to  $r_{def}/a = 0.2$ . Then we apply a fractional edge dislocation of order  $p$  is applied along the  $x$  axis, as shown in Figure 5. The dipole mode's frequency decreases as a function of the elongation parameter  $p$ ,<sup>8,24</sup> and it is desirable to start in the elongation process with a mode whose frequency is close to the edge of the air band, allowing enough space to achieve the optimum  $Q_{\perp}$  within the bandgap when the structure is tuned. In that case, the lateral confinement is preserved and  $Q_{\parallel}$  can be improved by increasing the number of photonic crystal layers around the defect. This is one of the reasons for reducing the defect hole radius to only  $0.2a$ . The other reason is our long-term goal, the photonic crystal cavity QED with neutral atoms,<sup>8</sup> for which we need a strong field intensity within an air hole large enough to place a neutral atom, without significant surface effects.

The symmetry of the PC surrounding the defect is broken by this deformation, which separates the doubly degenerate

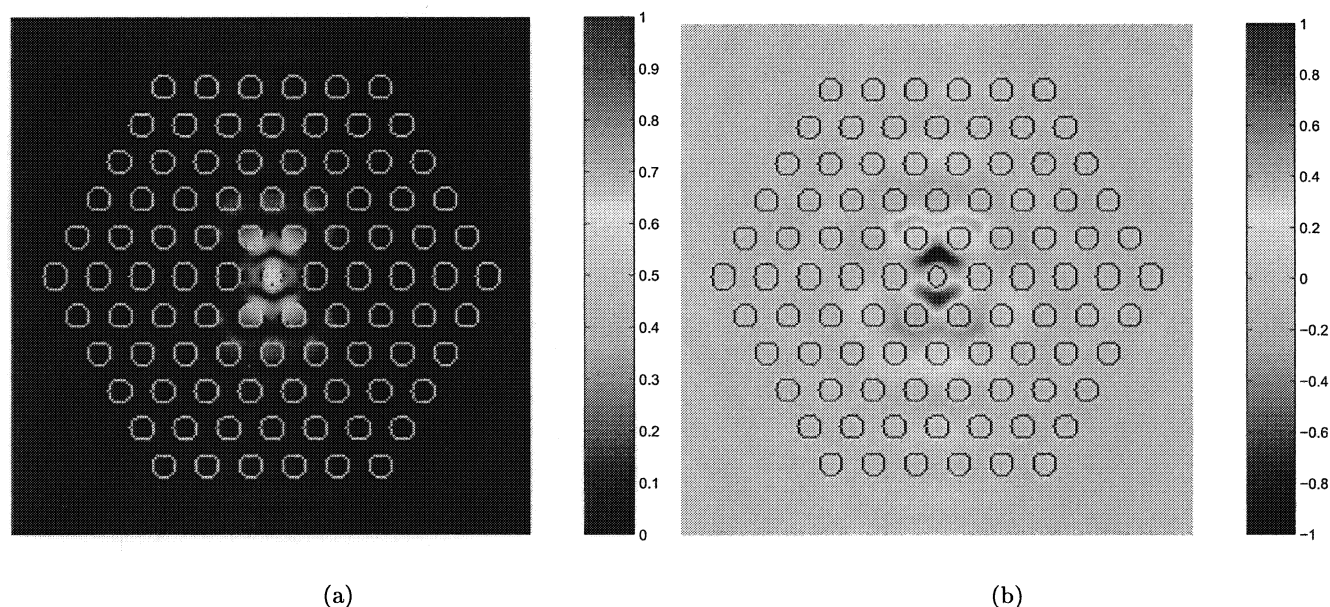


**Figure 6.** (a) Electric field intensity and (b)  $z$  component of magnetic field of the  $x$ -dipole mode, excited in the structure where the radius of the central PC hole is reduced and fractional edge dislocation of the order  $p = 2$  is added. Parameters of PC are described by the 1st set. The plotted intensity patterns are for the  $x$ - $y$  plane in the middle of the slab.

$x$  and  $y$  dipole modes in frequencies. The presented defect of the PC lattice spoils the  $Q$  factor of the  $y$ -dipole mode. On the other hand, for the  $x$ -dipole mode shown in Figure 6, this deformation leads to a significant  $Q$  improvement. Parameters of the  $x$ -dipole mode, as a function of the elongation parameter  $p$ , are shown in Figures 7 and 8. Therefore, by tuning  $p$ , the quality factor reaches values of over 10000. The mode volume  $V_{mode}$  does not change significantly with  $p$  and is approximately equal to  $0.5(\frac{\lambda}{n})^3$ . For structures operating at telecommunication wavelength  $\lambda = 1550nm$ , the elongation step  $\Delta p = 1$  corresponds to approximately  $23nm$ . From Figure 7, it follows that even when the elongation is accidentally detuned by  $20nm$  (i.e.,  $p$  changed from 2 to 3),  $Q$  still remains in the range of 10000. The insensitivity of  $Q$  to small variations in  $p$  is very important, since the small detuning in  $p$  during the fabrication process does not destroy properties of the structure. Thus, such structures are predicted to be relatively robust and manufacturable.

It is also interesting to note that the frequency of the mode decreases as  $p$  increases, even though the amount of low refractive index material increases. However, the net amount of low refractive index material does not matter. What matters more is where the low refractive index is positioned, relative to the unperturbed PC. The explanation of the

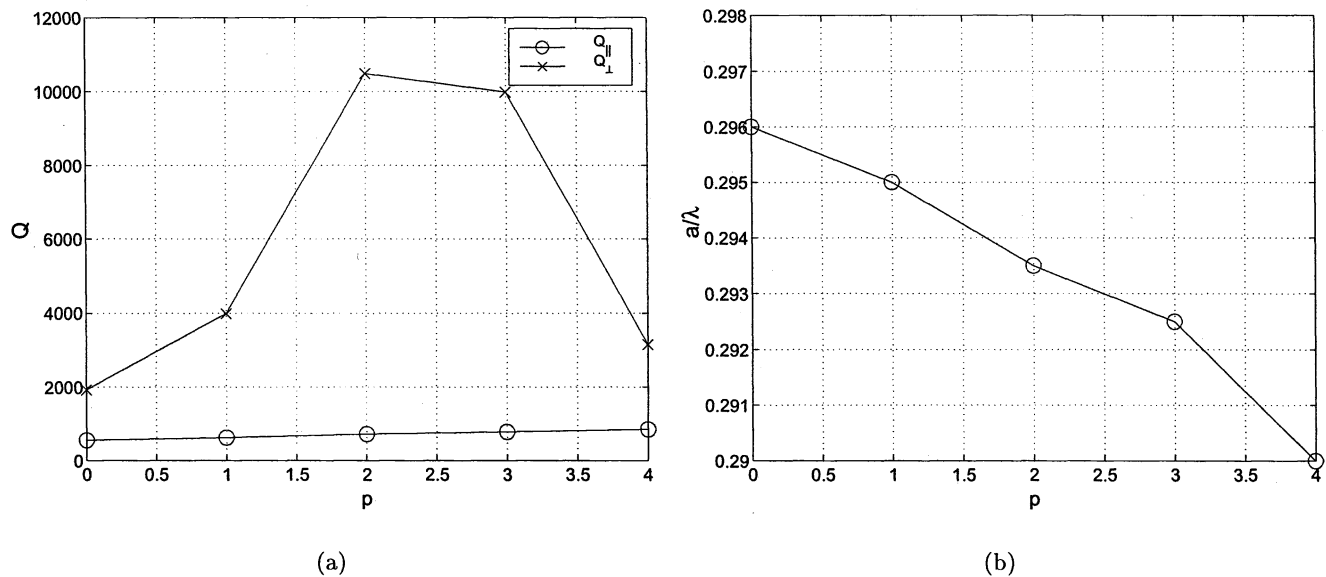


**Figure 7.** Parameters of the  $x$ -dipole mode in a single defect structure as a function of the elongation parameter  $p$ . The PC has the 1st set of parameters and the defect is formed by reducing the radius of the central hole to  $r_{def}/a = 0.2$ . (a)  $Q$  factors; (b) frequency in units  $a/\lambda$ .

decrease in frequency is very simple, if we recall the  $x$ -dipole mode pattern shown in Figure 6. This is a donor type defect mode, as previously stated, that concentrates its electric field energy density in low refractive index regions of the unperturbed PC. As  $p$  increases, layers of PC holes are moved away from the defect in the  $y$  direction. For example, the  $n$ -th layer of holes parallel to the  $x$  axis will now be positioned at  $y = \pm na\sqrt{3}/2 \pm p/2$ , instead of  $y = \pm na\sqrt{3}/2$ . Therefore, material with large refractive index (semiconductor) will now be positioned at places where the mode expects to "see" air, leading to a corresponding decrease in the mode's frequency.

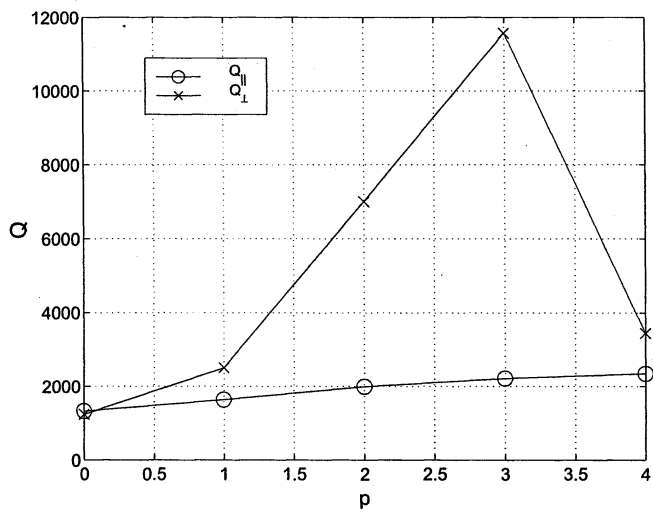
In Figures 7 and 8 one can observe that an increase in the elongation parameter  $p$  can be used to tune the  $Q_{\perp}$  factor of a mode, but it also leads to a decrease in the dipole mode's frequency. This implies that by increasing  $p$ , the mode is pulled deeper into the bandgap, away from the air band edge, which leads to its better lateral confinement and an increase in its  $Q_{\parallel}$ . Therefore, we can simultaneously achieve a reduction in vertical losses and an improvement in lateral confinement (i.e., an increase in both  $Q_{\perp}$  and  $Q_{\parallel}$ , and a reduction in the mode volume).

### 3. EXPERIMENT

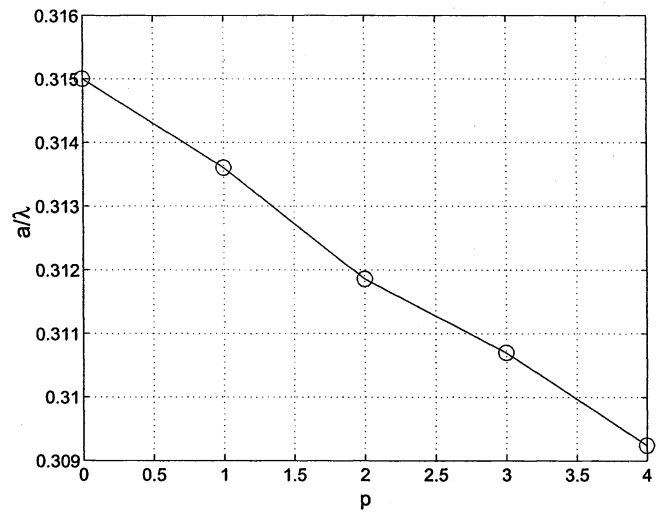
#### 3.1. Fabrication

Our group at Caltech has developed fabrication procedures for making optical microcavities based on planar PC, using a variety of semiconductor materials (Si, or III-V materials). For all material systems, the fabrication process starts by spinning of 100nm thick high molecular weight PMMA (polymethylmethacrylate) on top of the wafer. The PMMA layer is subsequently baked on a hot plate at 150°C for 20 minutes. A desired 2D PC pattern is beamwritten on the PMMA by electron beam lithography in a Hitachi S-4500 electron microscope. The exposed PMMA is developed in a 3:7 solution of 2-ethoxyethanol:methanol for 30 seconds. The pattern is then transferred into the membrane layer using the chemically assisted ion beam etching. Then, the sacrificial layer underneath the membrane is selectively attacked by acid dependent on the material system, resulting in a suspended membrane. Finally, the remaining PMMA may be dissolved in acetone.

The SEM pictures showing the top views of the fabricated nanocavities in Si or AlGaAs are shown in Figure 9.

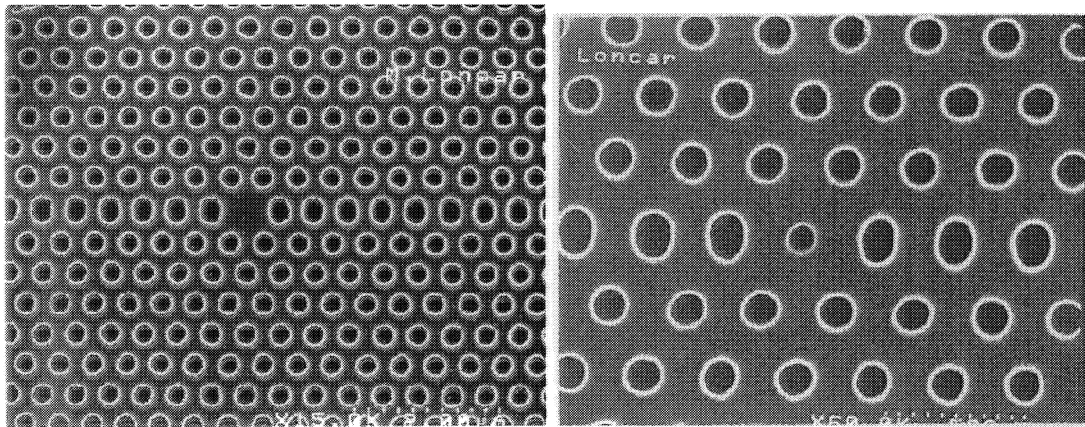


(a)



(b)

**Figure 8.** Parameters of the  $x$ -dipole mode in a single defect structure as a function of the elongation parameter  $p$ . The PC has the 2nd set of parameters and the defect is formed by reducing the radius of the central hole to  $r_{def}/a = 0.2$ . (a) Q factors; (b) frequency in units  $a/\lambda$ .



(a)

(b)

**Figure 9.** SEM pictures showing the top views of the fabricated structures in (a) Si and (b)  $Al_xGa_{1-x}As$ .

### 3.2. Characterization

We are presently working on characterization of passive cavities (made out of Si or AlGaAs), for the cavity QED experiments. However, using InAs quantum dots as internal photoluminescence sources, we have recently probed spectra of the presented nanocavities, and experimentally demonstrated Q factors as high as 2800 for the x-dipole mode in the structures with fractional edge dislocations.<sup>23</sup> An extremely good match between theory and experiment was observed, since the theoretically predicted Q value for this structure was around 4000. We have also experimentally observed the theoretically predicted tuning of Q values and frequencies of modes as a function of the elongation parameter p.

## 4. CONCLUSION

Optical nanocavities based on planar photonic crystals have been designed with Q factors over 10000 and mode volumes of the order of  $0.5 \left(\frac{\lambda}{n}\right)^3$ . Large spontaneous emission rate enhancements (60) and  $\beta$  factors (85%) can be achieved in these structures, which makes them excellent candidates for light sources based on the single mode spontaneous emission, with high quantum efficiency and broad modulation width.<sup>24</sup> We have also demonstrated theoretically that PC cavities can be designed for strong interaction with atoms trapped in one of the PC holes, which opens the possibility for using them in cavity QED experiments, or as building blocks of quantum networks. Structures have been fabricated and are presently being characterized for this purpose. Critical issues for further investigation include efficient coupling of light in and out of the PC nanocavities, as well as the significance of surface effects that could perturb atomic radiative structure within the small defect hole. The extremely small mode volume in these structures also poses an interesting theoretical question of how standard cavity QED models must be modified when the single-photon Rabi frequency greatly exceeds the atomic hyperfine spacing. Using InAs quantum dots as internal photoluminescence sources, we have recently probed spectra of our photonic crystal nanocavities, and experimentally demonstrated Q factors as high as 2800 in the structures where the theoretically predicted Q was equal to 4000.<sup>23</sup> The theoretically predicted tuning of Q values and frequencies of modes as a function of the elongation parameter p was also observed during the experiment.

## 5. ACKNOWLEDGMENTS

This work was supported by the Caltech MURI Center for Quantum Networks.

## REFERENCES

1. H. Haus and C. Shank, "Antisymmetric taper of distributed feedback lasers," *IEEE Journal of Quantum Electronics* **12**, p. 532, 1976.
2. E. Yablonovitch, "Inhibited Spontaneous Emission in Solid-State Physics and Electronics," *Physical Review Letters* **58**, pp. 2059–2062, May 1987.
3. S. John, "Strong localization of photons in certain disordered dielectric superlattices," *Physical Review Letters* **58**, pp. 2486–2488, 1987.
4. J. D. Joannopoulos, R. D. Meade, and J. N. Winn, *Photonic Crystals*, Princeton University Press, Princeton, New Jersey, 1995.
5. P. Villeneuve and M. Piché, "Photonic Bandgaps in Periodic Dielectric Structures," *Progress in Quantum Electronics* **18**, pp. 153–200, 1994.
6. C. Cheng, V. Arbet-Engels, A. Scherer, and E. Yablonovitch, "Nanofabricated three-dimensional photonic crystals operating at optical wavelengths," *Physica Scripta* **T68**, pp. 17–20, 1996.
7. M. Lončar, D. Nedeljković, T. Doll, J. Vučković, A. Scherer, and T. P. Pearsall, "Waveguiding at 1500nm using photonic crystal structures in silicon on insulator wafers," *Applied Physics Letters* **77**, pp. 1937–1939, Sept. 2000.
8. J. Vučković, M. Lončar, H. Mabuchi, and A. Scherer, "Design of photonic crystal microcavities for cavity QED," *Physical Review E* **65**, p. 016608, Jan. 2001.
9. O. Painter, R. Lee, A. Scherer, A. Yariv, J. O'Brien, P. Dapkus, and I. Kim, "Two-Dimensional Photonic Bandgap Defect Mode Laser," *Science* **284**, pp. 1819–1821, June 1999.

10. T. Yoshie, A. Scherer, H. Chen, D. Huffaker, and D. Deppe, "Optical characterization of two-dimensional photonic crystal cavities with indium arsenide quantum dot emitters," *Applied Physics Letters* **79**, pp. 114–116, July 2001.
11. P. Villeneuve, S. Fan, S. Johnson, and J. Joannopoulos, "Three-dimensional photon confinement in photonic crystals of low-dimensional periodicity," *IEEE Proceedings Optoelectronics* **145**, pp. 384–390, Dec. 1998.
12. D. Labilloy, H. Benisty, C. Weisbuch, C. Smith, T. Krauss, R. Houdre, and U. Oesterle, "Finely resolved transmission spectra and band structure of two-dimensional photonic crystals using emission from InAs quantum dots," *Physical Review B* **59**, pp. 1649–1652, Jan. 1999.
13. S. Noda, A. Chutinan, and M. Imada, "Trapping and emission of photons by a single defect in a photonic bandgap structure," *Nature* **407**, pp. 608–610, Oct. 2000.
14. M. Boroditsky, R. Vrijen, T. Krauss, R. Coccioli, R. Bhat, and E. Yablonovitch, "Spontaneous emission extraction and Purcell enhancement from thin-film 2-D photonic crystals," *Journal of Lightwave Technology* **17**, pp. 2096–2112, Nov. 1999.
15. J. Hwang, H. Ryu, D. Song, I. Han, H. Song, H. Park, Y. Lee, and D. Jang, "Room-temperature triangular-lattice two-dimensional photonic bandgap lasers operating at  $1.54\mu\text{m}$ ," *Applied Physics Letters* **76**, pp. 2982–2984, May 2000.
16. T. Baba, N. Fukaya, and A. Motegi, "Clear correspondence between theoretical and experimental light propagation characteristics in photonic crystal waveguides," *Electronics Letters* **37**, pp. 761–762, June 2001.
17. C. Smith, T. Krauss, H. Benisty, M. Rattier, C. Weisbuch, U. Oesterle, and R. Houdre, "Clear correspondence between theoretical and experimental light propagation characteristics in photonic crystal waveguides," *Journal of the Optical Society of America B* **17**, pp. 2043–2051, Dec. 2000.
18. J. Vučković, M. Lončar, and A. Scherer, "Design of photonic crystal optical microcavities," *Proceedings of the SPIE meeting Photonics West 2001, San Jose*, Jan. 2001.
19. S. Johnson, S. Fan, A. Mekis, and J. Joannopoulos, "Multipole-cancellation mechanism for high-Q cavities in the absence of a complete photonic bandgap," *Applied Physics Letters* **78**, pp. 3388–3390, May 2001.
20. E. Miyai and K. Sakoda, "Quality factor for localized defect modes in a photonic crystal slab upon a low-index dielectric substrate," *Optics Letters* **26**, pp. 740–742, May 2001.
21. J. Vučković, M. Lončar, H. Mabuchi, and A. Scherer, "Photonic crystal microcavities for strong coupling between an atom and the cavity field," *Proceedings of the LEOS 2000, Rio Grande, Puerto Rico*, Nov. 2000.
22. J. Vučković, M. Lončar, H. Mabuchi, and A. Scherer, "Optimization of Q-factor in microcavities based on free-standing membranes," *To appear in IEEE Journal of Quantum Electronics*, 2002.
23. T. Yoshie, J. Vučković, A. Scherer, H. Chen, and D. Deppe, "High quality two-dimensional photonic crystal slab cavities," *Applied Physics Letters* **79**, pp. 4289–4291, Dec. 2001.
24. J. Vučković, *Photonic crystal structures for efficient localization or extraction of light*, Ph.D. Thesis, California Institute of Technology, 2002.
25. M. Lončar, T. Doll, J. Vučković, and A. Scherer, "Design and fabrication of silicon photonic crystal optical waveguides," *Journal of Lightwave Technology* **18**, pp. 1402–1411, Oct. 2000.
26. E. Yablonovitch, T. Gmitter, R. Meade, A. Rappe, K. Brommer, and J. Joannopoulos, "Donor and acceptor modes in photonic band-structure," *Physical Review Letters* **67**, pp. 3380–3383, Dec. 1991.
27. O. Painter, J. Vučković, and A. Scherer, "Defect Modes of a Two-Dimensional Photonic Crystal in an Optically Thin Dielectric Slab," *Journal of the Optical Society of America B* **16**, pp. 275–285, Feb. 1999.